Biochimica et Biophysica Acta 1863 (2016) 3015–3026

Contents lists available at ScienceDirect

Biochimica et Biophysica Acta

journal homepage: www.elsevier.com/locate/bbamcr

Altered regulation of the Spry2/Dyrk1A/PP2A triad by homocysteine impairs neural progenitor cell proliferation

Luis G. Rabaneda [a,b], Noelia Geribaldi-Doldán [a,1], Maribel Murillo-Carretero [a,1], Manuel Carrasco [a], José M. Martínez-Salas [a,2], Cristina Verástegui [c], Carmen Castro [a,*]

[a] Área de Fisiología, Facultad de Medicina, Universidad de Cádiz, Spain
[b] Currently at Laboratorio de Neurobiología Celular, Centro de Investigación Médica Aplicada (CIMA), Universidad de Navarra, Pamplona, Spain
[c] Departamento de Anatomía, Facultad de Medicina, Universidad de Cádiz, Spain

ARTICLE INFO

Article history:
Received 22 March 2016
Received in revised form 13 September 2016
Accepted 22 September 2016
Available online 26 September 2016

Keywords:
neurogenesis
neural progenitor cells
homocysteine
Spry2
Dyrk1A
PP2A

ABSTRACT

Hyperhomocysteinemia reduces neurogenesis in the adult mouse brain. Homocysteine (Hcy) inhibits postnatal neural progenitor cell (NPC) proliferation by specifically impairing the fibroblast growth factor receptor (FGFR)-Erk1/2-cyclin E signaling pathway. We demonstrate herein that the inhibition of FGFR-dependent NPC proliferation induced by Hcy is mediated by its capacity to alter the cellular methylation potential. Our results show that this alteration modified the expression pattern and activity of Sprouty2 (Spry2), a negative regulator of the above mentioned pathway. Both elevated concentrations of Hcy and methyltransferase activity inhibition induced Spry2 promoter demethylation in NPC cultures leading to a sustained upregulation of the expression of Spry2 mRNA and protein. In addition, protein levels of two kinases responsible for Spry2 activation/deactivation were altered by Hcy: Spry2 kinase Dyrk1A levels diminished while Spry2 phosphatase PP2A increased, leading to changes in the phosphorylation pattern, activity and stability of Spry2. In conclusion, Hcy inhibits NPC proliferation by indirect mechanisms involving alterations in DNA methylation, gene expression, and Spry2 function, causing FGFR signaling impairment.,

1. Introduction

Hyperhomocysteinemia (HHcy) -abnormally elevated plasma levels of homocysteine (Hcy)- has been linked to the development of neurological disorders associated with neuronal loss such as Alzheimer's disease, vascular dementia or mild cognitive impairment [1–4]. Animal models of HHcy develop cognitive impairment [5] and, as we have previously shown, exhibit reduced adult brain neurogenesis [6].

Generation of neurons from neural stem cells (NSC) in the adult brain is activated in response to cellular demands in specific areas controlled by paracrine and endocrine signals, which create a neurogenic niche ([7,8] and reviewed in [9]). The two main neurogenic niches of the adult brain are the subventricular zone (SVZ) and the dentate gyrus of the hippocampus (DG). In these regions, NSC are active and divide with low frequency generating neural progenitor cells (NPC), highly proliferative cells that can produce precursors compromised with the neuronal fate (neuroblasts), which will differentiate into mature neurons [10,11].

One of the molecules that trigger NPC proliferation and neuronal differentiation, mainly within the DG, is the basic fibroblast growth factor (bFGF) [12–14]. Recent reports show that bFGF-stimulated proliferation of NPC is impaired by fluctuations in metabolites of the methylation pathway (see diagram in Fig. 1 H), including S-adenosylmethionine (SAM) and Hcy; these fluctuations negatively affect neurogenesis and hippocampus-dependent spatial memory as well. Hcy has been shown to specifically impair the bFGF receptor (FGFR)-induced, but not the epidermal growth factor receptor (EGFR)-induced, Erk1/2 phosphorylation and pErk1/2-stimulated upregulation of cyclin E in NPC [6,15], suggesting that the activity of one or more components of this signaling pathway might be compromised by elevated levels of Hcy; previous results also indicate that the effects of Hcy on adult neurogenesis are indirect, as a consequence of impaired methylation reactions resulting in the inhibition of NPC proliferation [6,15].

The FGFR-Erk1/2 signaling pathway is activated upon binding of bFGF to its receptor, resulting in the phosphorylation of FGFR and its immediate substrate FGFR substrate molecule 2 (FRS2). This facilitates the recruitment of the growth factor receptor bound protein 2 (Grb2) and the Son of Sevenless homolog protein 1 (Sos) to promote the activation of the small GTPases Ras/Raf and the cascade of MAP kinases, resulting in the phosphorylation of Erk1/2 (see diagram in Fig. 7). In NPC this pathway is active and the entrance of pErk1/2 in the nucleus enhances cyclin E expression and promotes proliferation [6]. To ensure

* Corresponding author at: Plaza Falla, 9, 11003 Cádiz, Spain.
E-mail address: carmen.castro@uca.es (C. Castro).
[1] Both authors contributed equally to the work.
[2] Currently at Servicio de Traumatología y Cirugía Ortopédica, Hospital Universitario Virgen del Rocío, Spain.

http://dx.doi.org/10.1016/j.bbamcr.2016.09.018
0167-4889/

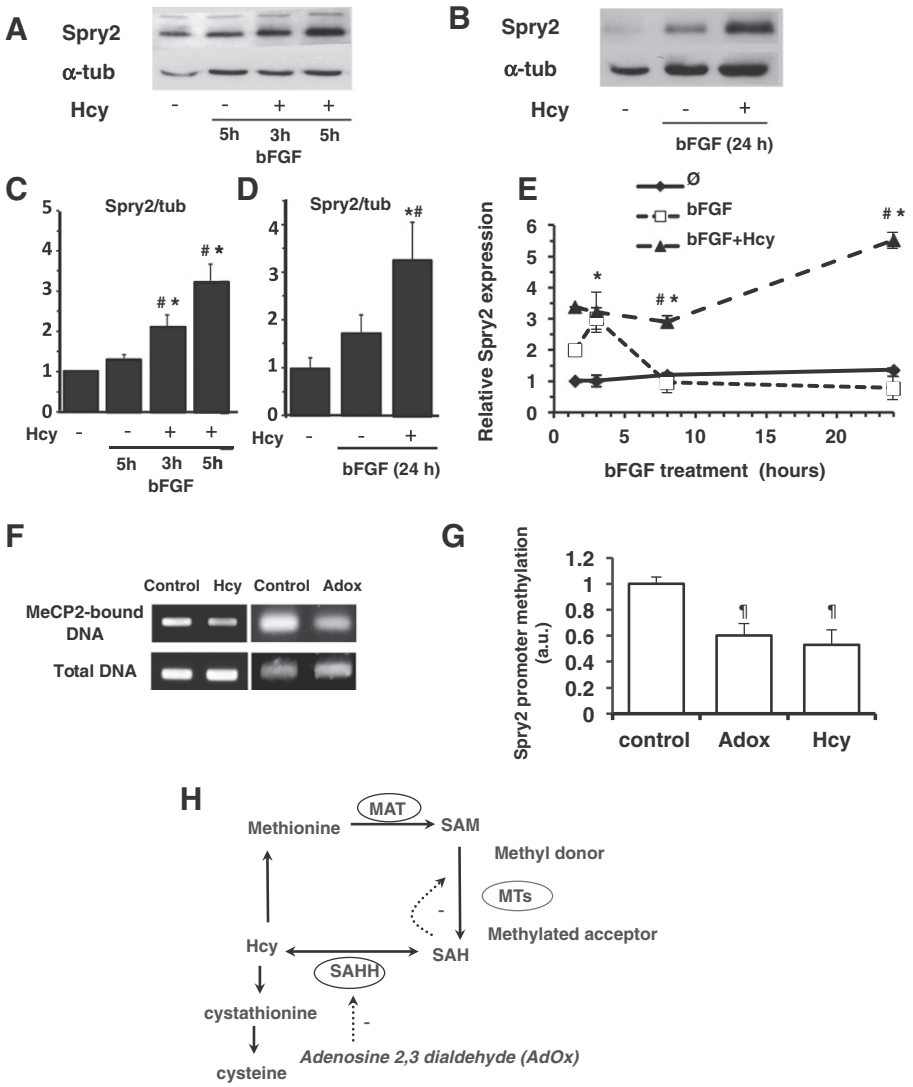

Fig. 1. Hcy upregulates Spry2 expression and induces Spry2-promoter demethylation in postnatal NPC. (**A-B**) Western blot representative autoradiographic images obtained after immunodetection of Spry2 and α-tubulin in NPC cultures grown under stated conditions. 100 μM Hcy was added at the time of seeding and bFGF (10 ng/mL) was added 1.5 h later; cells were lysed afterwards at the time points specified in the figures. (**C-D**) Densitometric quantification of bands from Spry2 western blots, as represented in A and B. Results are the average of 3 independent experiments; (*) means statistically significant with respect to none (no Hcy and no bFGF); (#) means statistically significant with respect to cultures stimulated with bFGF alone. (**E**) Normalized Spry2 mRNA expression 1.5, 3, 8 and 24 h after the addition of bFGF to NPC cultures. Hcy was added 1.5 h prior to bFGF; mRNA expression was quantified by qRT-PCR, using β-actin as normalizing gene. Fold increase has been calculated relative to initial time point (1.5 h) of the none. Results are the average of 3 independent experiments (*) means statistically significant with respect to none (no Hcy and no bFGF); (#) means statistically significant with respect to cultures stimulated with bFGF alone. (**F**) Representative photograph of an agarose gel electrophoresis showing the 140 bp fragment of Spry2 promoter illustrated in Fig. S3 amplified with primers described in the methods section. The region was amplified from MeCP2-bound DNA (upper panel) and total DNA (lower panel) obtained from control cultures (bFGF stimulation alone) and from cultures treated with bFGF + 100 μM Hcy or bFGF + 30 μM AdOx for 24 h. (**G**) MeCP2-bound Spry2 promoter was amplified from control, Hcy- or Adox-treated NPC (as described in F) and semi-quantified by qRT-PCR using total genomic Spry2 promoter amplification levels for normalization. Results are the average ± SE of three independent experiments (¶) means statistically significant with respect to control. (**H**) Schematic representation of the methionine cycle, also called *one carbon metabolism*, pinpointing the role of Hcy and AdOx in methyltransferase activity regulation.

appropriate responses that are critical for normal cell function, this cascade is negatively regulated in terms of both duration and intensity by the adaptor protein Sprouty homolog 2 (Spry2) [16]. Spry2 binds to Growth Factor Receptor Bound Protein 2 (Grb2), interfering with the formation of the Grb2-Sos complexes required for the activation of Erk1/2. Spry2 activity can be modulated by posttranslational changes in its phosphorylation pattern, although the phosphoregulation of Spry2 activity is rather complex and involves Tyr, Ser and Thr phosphorylation by several kinases [17] including casein kinase 1, Mnk1, Tesk and Dyrk1A [17–20] as well as dephosphorylation by protein phosphatase 2 A (PP2A) [21] (see diagram in Fig. 7). Phosphorylation of tyrosine residues within the Spry2 molecule modulates its activity and its capacity to repress the FGFR signaling cascade. Specifically Tyr55 can either facilitate its binding to E3 ubiquitin-protein ligase (c-Cbl) and its rapid degradation via the proteasome, thus facilitating FGFR-Erk1/2 signaling (reviewed in [22]) or its binding to PP2A. In addition, phosphorylation of Spry2 in Thr75 by Dyrk1A avoids Spry2 inhibition of FGFR-MAPK signaling pathway [20]. On the contrary, dephosphorylation of Spry2 mediated by the Ser/Thr protein phosphatase 2 A (PP2A) is a prerequisite for Erk1/2 inhibition downstream of FGFR [21]. Cellular Spry2 expression is tightly regulated both at the transcriptional and the posttranslational level [23], and changes in Spry2 concentration and phosphorylation in several cell lines lead to changes in cell proliferation [24–26].

The Dyrk1A gene is located on chromosome 21 and triplicated in Down syndrome [27]. A correct dosage of Dyrk1A is essential for mammalian brain development, mainly for corticogenesis. Dyrk1A regulates G1 and cell cycle length, as well as asymmetric or neurogenic divisions of intermediate neural progenitor cells. Hence, this protein determines

the fate of neural stem cells during embryonic development [28–31] and alterations in Dyrk1A dosage leads to developmental disorders of the CNS such as Down syndrome.

Spry2 and Dyrk1A expression is altered in the brain of mice that are hyperhomocysteinemic as a result of cystathionine ß synthase deficiency [32]. Hcy is an intermediate in the methionine cycle (Fig. 1 H), which is the biochemical path for the production of S-adenosylmethionine (SAM), the universal methyl donor [33]. Donation of SAM methyl groups in transmethylation reactions produces S-adenosylhomocysteine (SAH), which is an allosteric inhibitor of methyltransferases (MT). SAH is then hydrolyzed into adenosine (Ado) and Hcy in a reversible reaction. Elevated concentrations of either Ado or Hcy lead to accumulation of SAH, which inhibits MT. Thus, the cellular methylation potential is determined by the ratio SAM/SAH, and impaired DNA or protein methylation in the presence of elevated Hcy might be the ultimate cause underlying misregulation of FGFR signaling in NPC.

In here, we have deepened into the effects of Hcy on specific components of the FGFR-Erk1/2 pathway in NPC. We show that the antiproliferative effect of Hcy in these cells is indeed mediated by its capacity to inhibit methylation reactions leading to hypomethylation of the Spry2 promoter and upregulation of both Spry2 mRNA and protein. We also show that Hcy downregulates Spry2 kinase Dyrk1A, and upregulates Spry2 phosphatase PP2A in NPC, all of which leads to accumulation of the active form of Spry2, responsible for repressing FGFR-Erk1/2 signaling and bFGF-induced NPC proliferation. Finally, we have also checked the pathophysiological relevance of these findings in a mouse model of HHcy.

2. Materials and Methods

2.1. Materials

For *in vitro* studies, a stock solution of 100 mM DL-Hcy was prepared from Hcy thiolactone (Sigma-Aldrich; St. Louis MO USA) as previously described [34]; double amounts of DL-Hcy were added to cell culture wells in order to obtain each concentration of L-Hcy. For *in vivo* studies, DL-Hcy was directly purchased from Sigma-Aldrich (St Louis MO, USA). Adenosine dialdehyde (AdOx), okadaic acid, harmine and alkaline phosphatase were purchased from Sigma-Aldrich.

2.2. Animal Subjects

Adult and 7-day postnatal CD1 mice were used throughout this study. Adult mice were housed individually at temperature (21–23 °C) and light (LD 12:12) controlled conditions with free access to food and water. Mice were fed AO4 standard maintenance diet (SAFE, Épinay-sur-Orge, France). Care and handling of animals were performed according to the Guidelines of the European Union Council (86/609/EU), following the Spanish regulations (RD 53/2013) for the use of laboratory animals.

2.3. SVZ cell isolation and culture

NPC for *in vitro* studies were obtained from the SVZ of CD1 postnatal mice (P7) following the procedure reported previously [35], and maintained as neurosphere cultures as described before [6]. Neurospheres were mechanically disaggregated in DF12 medium supplemented with B27 and growth factors bFGF and EGF. Single cells were re-seeded on 25-cm^2 low-adherence flasks at a 100 cells/μL density, and passaged every two days.

2.4. Immunocytochemistry

Cells dissociated from neurospheres were seeded at a density of 100 cell/μL onto poly-L-ornithine (PLO)-coated 8-well glass slide chambers (Nalgene Naperville, IL, USA) and maintained for 48 h in defined medium supplemented with bFGF (10 ng/mL). Hcy, AdOx and the different treatments were added at the time of seeding 1–1.5 h before bFGF addition, and left for different times as indicated in figure legends. Immunocytochemistry was performed as described before [6]. Antibodies used were: rabbit polyclonal anti-Ki67 (dilution 1:1000) (Vector, Burlingame, CA), and goat anti-rabbit IgG (H + L) labeled with either AlexaFluor 568 (dilution 1:1000) or 488 (dilution 1:1000) (Invitrogen, Carlsbad, CA). Nuclei were counterstained for 10 min with 0.1 mg/L DAPI (4′,6-diamidino-2-phenylindole). $Ki67^+$ cells were counted under a BX60 epifluorescence microscope (Olympus, Hamburg, Germany) and expressed as percentage of the total number of cells, determined by DAPI staining. Quantification was performed in 12 predetermined visual fields per well and 3 wells per condition. Experiments were repeated a minimum of 3 times and results were expressed as the mean ± SEM.

2.5. Immunoblot analysis

Cells from neurospheres were disaggregated and incubated for 1–1.5 h in the presence or absence of 100 μM L-Hcy or 30 μM AdOx and then other treatments were added as indicated in figure legends. The growth factor bFGF was added last and cultures were processed at different time points afterwards as indicated in the figure legends. Cells were lysed with ice-cold Cell Lysis Buffer containing phosphatase and protease inhibitors (all from Cell Signaling Technology, Boston, MA, USA) with additional 1 mM phenylmethylsulfonylfluoride (PMSF). Supernatants were collected after centrifugation (16,000 x g) and their protein concentration was measured. Equal amounts (50 μg) of total protein from each cellular extract were used for immunoblot detection. We used the following antibodies: anti-pErk1/2 Tyr 202 and Tyr 204 (1:500), anti-Erk1/2 (1:100), anti-pFRS2 (1: 250) and anti-PP2Ac (1:1000) were from Cell Signaling Technology, Inc. (Boston MA, USA); anti-cyclin E (1: 500) was from Santa Cruz Biotechnologies (Santa Cruz, CA, USA), anti-Spry2 (1:1000) was from Abcam (Cambridge, UK), anti-Dyrk1A (1:750) was from Abnova (Taipei, Taiwan), and anti-α-tubulin (1:1000) was from Sigma-Aldrich (St. Louis MO, USA). Immunodetection was performed using the Western Breeze chemiluminescence kit (Invitrogen, Carlsbad, CA), following manufacturer's instructions.

Tissue samples were obtained as follows: mice were sacrificed by cervical dislocation and brains were immediately removed. Hippocampal tissues were dissected out and immediately frozen in liquid nitrogen. Later on, tissues were homogenized in Kinase Buffer (Cell Signaling Technology, Boston, MA) containing protease and phosphatase inhibitors with additional 1 mM PMSF.

2.6. RAS GTPase activity assays

Ras GTPase activity was analyzed using the "Active Ras Pull-Down and Detection Kit" (Thermo Scientific, Rockford, IL, USA), which consists in the pull down of RAS-GTP triggered by the Ras-GTP-binding domain of Raf1 bound to glutathione agarose. Positive (GTPγS) and negative (GDP) control conditions were used to validate the assay. A density of 1000 cells/μL was seeded per condition to perform this assay. 200 μM DL-Hcy was added at the time of seeding and bFGF was added 1.5 h later; cells were lysed 3 h after addition of bFGF. Immunoprecipitated Ras-GTP was analyzed by SDS-PAGE and western blot using the monoclonal anti-Ras antibody (1:250) included in the kit. Total Raf1 was detected in total homogenate with an anti-Raf1 antibody (1:500) (Upstate Cell Signalling, NY) and used as a loading control.

2.7. RNA isolation and reverse transcription

Total RNA was isolated using the "RNeasy mini kit" (Qiagen, Germany) according to manufacturer's instructions. First-strand cDNA was prepared from total RNA using random primers and the SuperScript

II Reverse Transcriptase Kit, in the presence of RNaseOUT ribonuclease inhibitor (all from Invitrogen, Carlsbad, CA, USA).

2.8. PCR and real time-PCR

Spry2 and Dyrk1A mRNAs were semi-quantified by real time-PCR, using the iQ SYBR Green Supermix system and a MiniOpticon thermal cycler (Bio-Rad, Hercules, CA, USA) according to manufacturer's instructions. β-actin mRNA levels were used for normalization. Reactions were run in duplicate, and a minimum of 3 different cultures were used independently for each determination. Amplification specificity was confirmed by melting-curve analysis of the PCR products. The relative abundance of mRNA in each sample was calculated as $2^{-\Delta\Delta Ct}$ (published in Applied Biosystems Bulletin No. 2, P/N4303859) and validated [36]. No signal was detected in non-template or non-RT controls. Primers used to detect Spry2 (Fw: 5´-GAGAGGGGTTGGTGCAAAG; Rw: 5´-CTCC ATCAGGTCTTGGACGT), Dyrk1A (Fw: 5´-ATCCGACGCACCAGCATC; Rw: 5´-AATTGTAGACCCTTGGCCTGGT) and β-actin (Fw: 5´-GAAATCGTGGC TGACATCAAAG; Rw: 5´-TGTAGTTTCATGGATGCCACAG) were synthesized by Sigma-Aldrich (St Louis, MO, USA).

2.9. Spry2 promoter methylation assays

Methyl-CpG rich regions of the mouse Spry2 promoter were selected from sequence NC_000080.5; Gen ID: NM0011897.3; base pairs 106,295,065–106,297,259 (Supplementary Fig. S3) using the "epigenomics" tool (http://www.ncbi.nlm.nih.gov/epigenomics), which highlights the regions of mouse Spry2 promoter in which the percentage of methyl-CpG rich sequences are >85% in sperm, blood and adult cerebellum. Spry2 promoter methylation was analyzed using the promoter methylation PCR kit from Affymetrix (Santa Clara, CA; USA), which is based on the *Mse*I digestion of genomic DNA followed by the pull down of MseI-digested methyl-CpG fragments using the methyl binding domain of MeCP2 followed by PCR analysis of the MeCP2-precipitated DNA fragments, using specific primers to amplify a methyl CpG-rich region. In order to find the adequate primers for PCR analysis, an *Mse*I restriction analysis was performed of the sequence comprising base pairs 106,295,963–106,297,259 of NM011897.3 and a primer set was designed to amplify a CpG-reach region (PR1) within this sequence located between two *Mse*I sites, as represented in Supplementary Fig. S3 (Fw: 5′ GCTTTCTCTCATCGACCAGG; Rw: 5′ CCGGGATAG ATGACCTCCCTT). In addition, a set of primers was designed to amplify a region in exon 1 (ER 2) also located between two *Mse*I sites to be used as a negative control (Fw: 5′ AGCACGGGTTGTCAGCACA; Rw: 5′CAGGTG TGAGGACTGCGGCA).

Genomic DNA from 5 million cells per condition was isolated using DNeasy mini kit (Qiagen, Germany) and 4 μg of this DNA were digested with the restriction enzyme MseI for 2 h at 37 °C. MseI-digested DNA was pulled down with MeCP2 and PCR or qRT-PCR was performed to test the presence of PR1 and ER2 in MeCP2-bound DNA and in the supernatant. ER2 was PCR-amplified as a negative control.

2.10. Spry2- and Dyrk1A- pcDNA3.3 plasmid constructs

Mouse Spry2 (GB Accession NM_011897) and Dyrk1A (GB Accession NM_007890) cDNAs were amplified by PCR from mRNA after reverse transcription. Primers used to amplify Spry2 (Fw: 5′-ATGGAG GCCAGAGCTCAGAGTGGC; Rw: 5′- CTATGTCGGCTTTTCAAAGTTCCT) and Dyrk1A (Fw: 5´-ATGCATACAGGAGGAGAGACT; Rw: 5´ TCACGA GCTAGCTACAGGACT), were synthesized by Sigma-Aldrich (St Louis MO, USA). PCR amplification products were analyzed by agarose gel electrophoresis, purified and ligated into pcDNA3.3-topo (Invitrogen, Carlsbad, CA, USA) according to manufacturer's instructions.

2.11. NPC transfection with pcDNA3.3 plasmid constructs

Transfection of plasmids was performed using Lipofectamine 2000 following manufacturer's instructions. Following transfection cells were left for 24 h in the presence of treatments indicated in the figure legends and then processed for immunocytochemistry to detect Ki67 or western blot to detect Spry2.

2.12. Animal model of HHcy

An animal model of HHcy was established by implanting Hcy-releasing osmotic minipumps to adult mice (38–42 g). Under general anesthesia (Ketamine 120 mg/kg; Xylacine 20 mg/kg), an osmotic minipump (Alzet, model number 2002, Palo Alto, CA, USA) was placed subcutaneously in the subscapular fossa region. Minipumps were filled with 200 μL of either vehicle (sterile filtered dH_2O) or 100 mM L-Hcy, to be released over 2 weeks (equivalent to 1 mg Hcy/day) [6].

2.13. Measurement of total plasma Hcy levels (tHcy)

Immediately prior to sacrifice, blood samples collected by puncture of the left ventricle were centrifuged and plasma was kept frozen at −20 °C until Hcy measurement. tHcy levels were determined using an enzymatic assay (Axis-Shield Diagnostics; Dundee, UK) and measurements were recorded at 340 nm and 37 °C in a BioTek PowerWave HT Microplate Spectrophotometer (BioTek Instruments, Winooski, VT, USA). Control plasma samples with normal and abnormal ranges of Hcy were used to calibrate the assay.

2.14. Statistical Analysis

Statistical analyses of both *in vitro* and *in vivo* experiments were performed using ANOVA and Bonferroni *post-hoc* test *t*, when more than one treatment group was compared with the control situation. Student's t-test was used only when one treatment group was compared versus control. The differences were considered significant when $p < 0.05$.

3. Results

3.1. Homocysteine inhibits FGFR signaling in postnatal neural progenitors by mechanisms acting upstream of Ras

As a first approach to understand which components within the FGFR-Erk1/2 signaling cascade were specifically altered in the presence of elevated levels of Hcy, we analyzed the phosphorylation of the FGFR substrate FRS2 and the activity of Ras/Raf proteins. Treatment of NPC cultures with 100 μM Hcy induced no effect on the phosphorylation of FRS2 (Fig. S1 A-B). However, a significant decrease on GTP-bound Ras was observed (Fig. S1 C-D), which suggested that Hcy was exerting its effect on molecules participating in the bFGF signaling cascade upstream of Ras and downstream of FRS2. This pointed out the possibility that the FGFR signaling regulator Spry2 was altered in the presence of elevated Hcy.

3.2. Transient bFGF-driven upregulation of Spry2 expression

The abundance of Spry2 protein in control cultures and in cultures treated with 100 μM Hcy was assayed by western blot, at different time points after bFGF addition. Stimulation of NPC cultures with bFGF for 5 h (Fig. 1 A, C) or 24 h (Fig. 1 B, D) resulted in only a moderate, non-statistically significant increase on Spry2 protein abundance; however, in cultures pre-treated with Hcy, Spry2 protein expression was significantly upregulated, as measured at 3, 5 and 24 h after bFGF stimulation (Fig. 1 A-D).

We next sought to determine whether the observed changes in Spry2 protein levels correlated with parallel changes in Spry2 mRNA. For this purpose, Spry2 mRNA expression was analyzed in NPC cultures stimulated with bFGF, either alone or in the presence of Hcy. bFGF stimulation of NPC cultures induced a transient upregulation of Spry2 mRNA reaching a maximum (a 3 fold increase compared to unstimulated cultures) 3 h after bFGF addition. After this peak of expression, Spry2 levels declined, reaching basal levels 8 h after bFGF was added. In contrast, when NPC cultures were in the presence of Hcy, Spry2 mRNA levels persisted elevated during the first 8 h of bFGF treatment, and even increased further up to 5 fold 24 h after bFGF addition (Fig. 1 E).

3.3. CpG islands within the Spry2 promoter become hypomethylated after exposure to Hcy

Elevated Hcy might imbalance the SAM/SAH ratio, impairing Spry2 promoter methylation and facilitating Spry2 gene transcription. In order to test this hypothesis, we analyzed the methylation state of Spry2 promoter in DNA isolated from bFGF-stimulated NPC, cultured in the absence or presence of 100 μM Hcy for 24 h. Methyl-CpG groups were pulled down from digested DNA extracts using recombinant methyl-CpG binding protein 2 (MeCP2). These MeCP2-bound DNA fractions were used as templates for PCR amplification of a small Spry2 promoter fragment rich in CpG islands, revealing that the proportion of this Spry2 promoter fragment bound to MeCP2 (and thus the amount of methyl-CpG groups on it) was significantly reduced in Hcy-treated samples, when compared to non-treated controls (Fig. 1 F-G). Consequently, in order to verify that the effect of Hcy on Spry2 promoter methylation was mediated by its capacity to imbalance the SAM/SAH ratio and, therefore the cellular methylation potential, we treated NPC cultures for 24 h with the adenosine analogue adenosine 2,3-dialdehyde (AdOx), which inhibits S-adenosylhomocysteine hydrolase (SAHH) leading to SAH accumulation (see diagram in Fig. 1 H). As expected, the amount of MeCP2 bound to Spry2 promoter was lower in cultures treated with 30 μM AdOx than in non-treated controls (Fig. 1 G), suggesting that SAH-mediated methyltransferase inhibition underlies Spry2 promoter demethylation and facilitates its gene transcription.

3.4. The adenosine analogue AdOx reduces FGFR-Erk1/2 signaling, cyclin E expression and cell proliferation in NPC cultures

It was next tested whether AdOx mimicked the previously-reported effects of Hcy on NPC proliferation, Erk1/2 phosphorylation, and cyclin E expression. As previously observed with Hcy treatment, AdOx addition to NPC cultures reduced the percentage of $Ki67^+$ cells, thus inducing an antiproliferative effect (Fig. 2 A, B) that was concomitant with a 50% reduction in bFGF-dependent Erk1/2 phosphorylation and cyclin E expression (Fig. 2 C-E).

3.5. Hcy alters the posttranslational phosphorylation pattern of Spry2

As previously shown in Fig. 1 (A-E), NPC cultures that had been stimulated for short times (3–5 h) with bFGF alone showed a transient increase on Spry2 mRNA levels, which did not traduce into increased protein expression. In contrast, the concomitant addition of Hcy to the cultures, albeit yielding similar Spry2 mRNA levels at this short time of treatment, resulted in increased Spry2 protein expression. These results suggested that Spry2 might be rapidly degrading in the presence of bFGF, and that Hcy addition could be inducing some kind of posttranslational modifications, such as phospho/dephosphorylation, leading to Spry2 protein stabilization. In order to visualize phospho-Spry2 and dephospho-Spry2, NPC cultures were treated with the proteasome

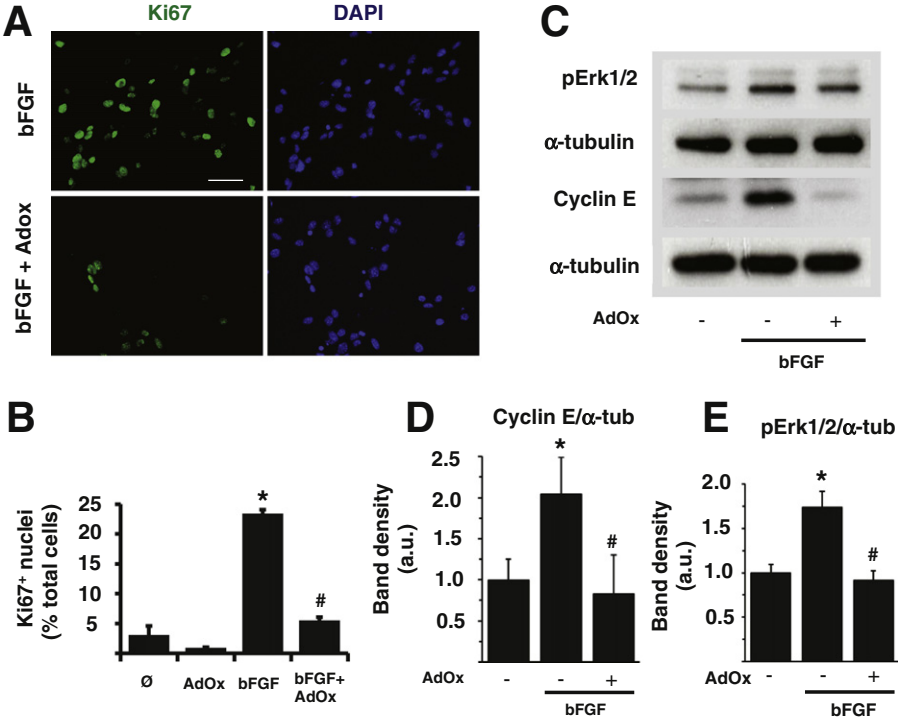

Fig. 2. AdOx mimics Hcy-induced inhibition of NPC proliferation, Erk1/2 phosphorylation and cyclin E expression. (**A**) Representative fluorescence microscopy images showing immunodetection of the proliferation marker Ki67 (green) and nuclear DAPI staining (blue) on NPC cultures attached onto poly-L-ornithine (PLO) and treated for 48 h with bFGF in the presence and absence of the methyltransferase inhibitor AdOx (30 μM). Scale bar: 50 μm. (**B**) Percentage of $Ki67^+$ cells in NPC adhered onto PLO and cultured for 48 h in the different experimental conditions indicated. **(C)** Representative autoradiographic images obtained after immunodetection of pErk1/2, α-tubulin and cyclin E. Cultures were treated with Adox or vehicle for 1.5 h before the addition of bFGF. Cells were lysed 4 h after addition of bFGF (**D-E**) Densitometric quantification of pErk1/2 and cyclin E bands normalized to the corresponding α-tubulin bands, as represented in C. Results are the average ± SE of 3 independent experiments; (*) means statistically significant with respect to control, (#) means statistically significant with respect to bFGF-stimulated cultures.

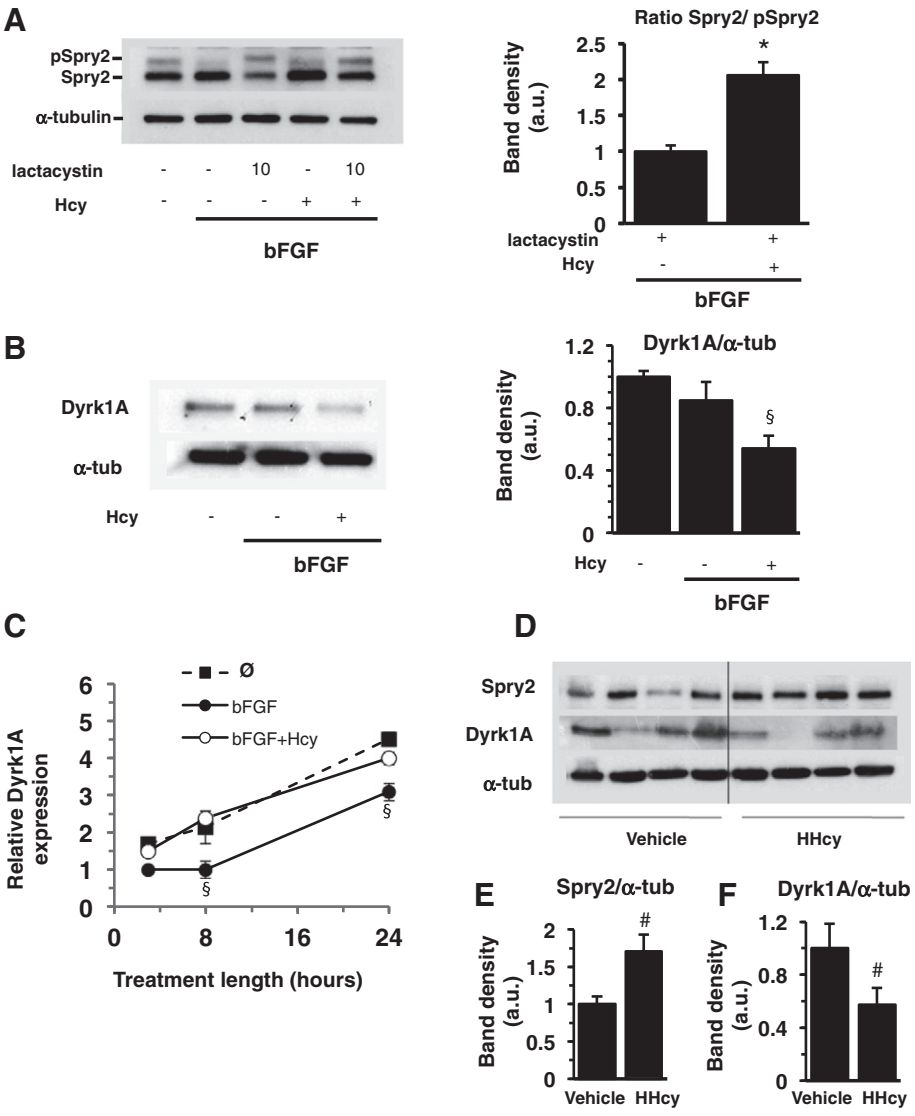

Fig. 3. Hcy favors Spry2 dephosphorylation and reduces Spry2 kinase Dyrk1A protein levels. (**A**) Representative autoradiographic images obtained after immunodetection of Spry2 and α-tubulin in the indicated culture conditions, and densitometric quantification of bands expressed as the ratio Spry2/phosphoSpry2 in lactacystin-treated bFGF-stimulated cultures in the presence and absence of Hcy. Cells were treated with 100 μM Hcy and 10 μM lactacystin 1.5 h before bFGF stimulation, and lysed 4 h after addition of bFGF. Results are the average of 3 independent experiments. (**B**) Representative autoradiographic images obtained after immunodetection of the Spry2 kinase Dyrk1A and α-tubulin in the indicated culture conditions, and densitometric quantification of bands expressed as the ratio Dyrk1A/α-tubulin. Cells were treated with or without 100 μM Hcy 1.5 h before addition of bFGF, and lysed 3 h after addition of bFGF. Results are the average ± SE of 3 independent experiments. (**C**) Relative Dyrk1A mRNA expression in control, bFGF-stimulated and Hcy-treated bFGF-stimulated cultures, after 3, 8 and 24 h of bFGF stimulation. 100 μM Hcy was added 1.5 h before addition of bFGF, mRNA expression was quantified by qRT-PCR, using β-actin as normalizing gene. Fold increase has been calculated relative to the initial time point (3 h) of the none condition. (**D**) Representative autoradiographic images obtained after western blot immunodetection of Spry2, Dyrk1A and α-tubulin in the hippocampus of vehicle- and Hcy-treated mice. (**E, F**) Densitometric quantification of Spry2 and Dyrk1A immunodetected bands using a-tubulin as loading control. Results are average ± SE of four animals in each experimental group. (*) means statistically significant compared to control the Hcy-devoid condition, (§) means statistically significant compared to the rest of treatments shown and (#) means statistically significant compared to vehicle.

inhibitor lactacystin to avoid proteasomal degradation of the phosphorylated Spry2 form [21,37], and it was found that an additional Spry2 band with a higher molecular weight appeared after western blot immunodetection with an anti-Spry2 antibody (Fig. S2). This additional Spry2 band disappeared after treatment with alkaline phosphatase, indicating that it was indeed a phosphorylated form of Spry2.

We next analyzed the effect of Hcy on Spry2 phosphorylation, using 10 μM lactacystin to inhibit proteasomal degradation of phospho-Spry2 (Fig. 3 A). In the presence of Hcy, the proportion of dephosphorylated Spry2 augmented in 2-fold compared to control cultures (Fig. 3 A), suggesting that the increase on Spry2 protein observed after short-term treatment with Hcy could be a consequence of a reduction in Spry2 phosphorylation.

In order to understand the mechanisms underlying the elevated dephospho-Spry2 observed in the presence of Hcy, we studied the expression of the Spry2 kinase Dyrk1A and the Spry2 phosphatase PP2A in NPC cultures subjected to Hcy treatment.

3.6. Dyrk1A expression is downregulated in the presence of Hcy

Dyrk1A protein expression was analyzed by western blot in NPC cultures. A basal expression of Dyrk1A could be observed that was not significantly changed by a 3 h-stimulation with bFGF. However, pre-treatment of bFGF-stimulated NPC with 100 μM Hcy reduced Dyrk1A expression by 50% (Fig. 3 B). This reduction in Dyrk1A protein was not concomitant with a reduction in Dyrk1A mRNA (Fig.3 C), suggesting that Dyrk1A protein downregulation mediated by Hcy occurred at the posttranslational level. Surprisingly, a reduction in Dyrk1A mRNA levels was observed in NPC cultures stimulated with bFGF, although this reduction could only be observed in the absence of Hcy (Fig. 3 C).

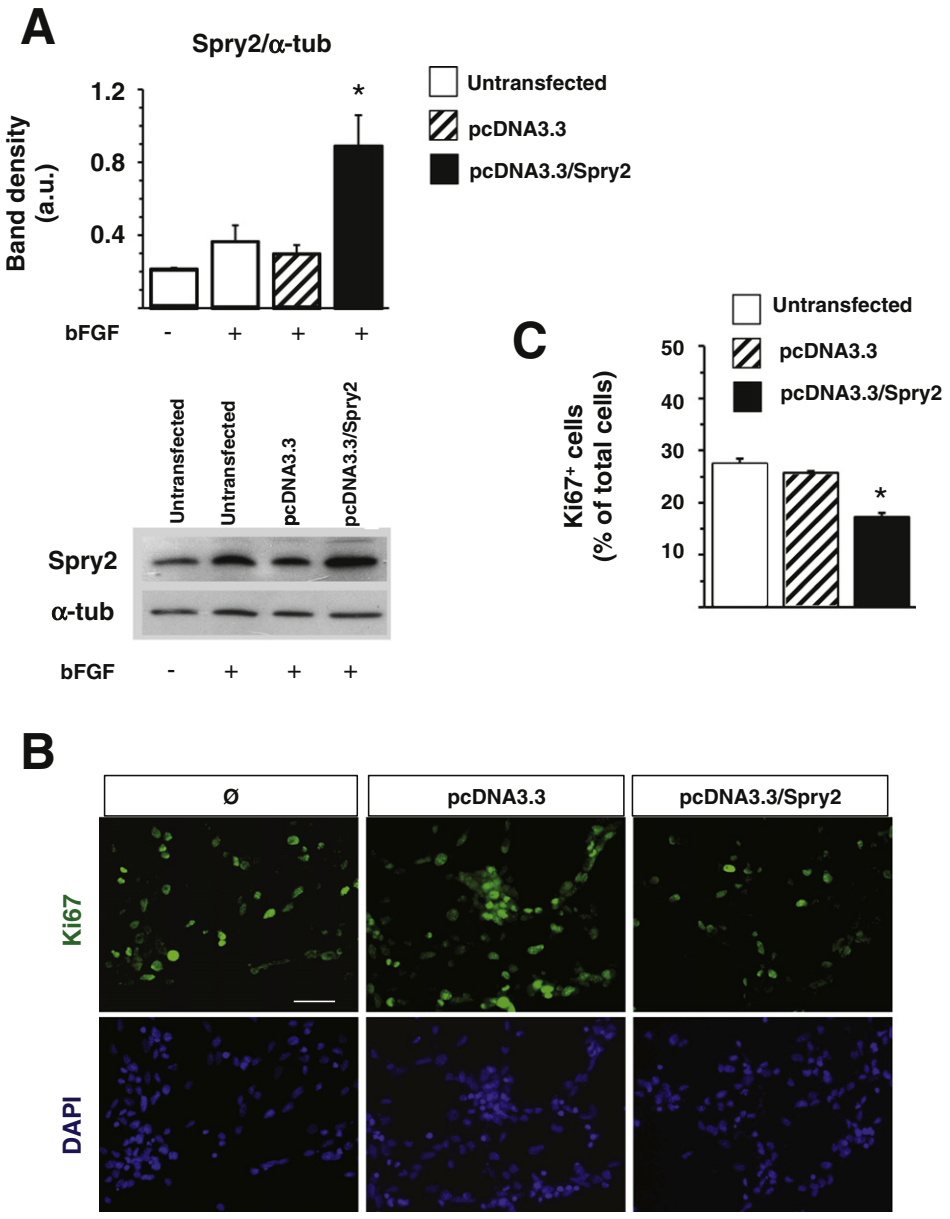

Fig. 4. Spry2 overexpression inhibits NPC proliferation. NPC were transfected with a plasmid containing the Spry2 cDNA, and controls were made in the absence of transfection or by transfecting the empty plasmid (pcDNA3.3). Cultures were treated as indicated. (**A**) Representative autoradiographic images obtained after immunodetection of Spry2 and α-tubulin in cultures transfected and treated as indicated for 48 h; the graph shows the densitometric quantification of bands. Results are the average of 3 independent experiments. (**B**) Representative fluorescence microscopy images showing immunodetection of Ki67 (green) and DAPI staining (blue) of bFGF-treated NPC cultures attached onto PLO that were either untransfected (bFGF), or transfected with an empty pcDNA3.3 vector or a pcDNA3.3-Spry2 vector. Scale bar: 50 μm. (**C**) Percentage of $Ki67^+$ cells in NPC cultures in the different culture conditions explained in B, as indicated. Data correspond to the average ± SE of three independent experiments performed in triplicates; (*) means statistically significant compared to the rest of groups.

3.7. Hyperhomocysteinemic mice exhibit high levels of Spry2 and low levels of Dyrk1A proteins in neurogenic regions of the brain

We next sought to determine whether chronic systemic HHcy altered the expression of Spry2 and Dyrk1A in neurogenic regions of the brain. To answer this, we generated hyperhomocysteinemic mice by implanting subcutaneous osmotic minipumps containing Hcy to be slowly delivered throughout 2 weeks, which resulted in moderate hyperhomocysteinemia (tHcy = 10.5 ± 2.8 μM in control *vs.* 29.7 ± 11.9 μM in Hcy-treated mice). Then, the expression of both proteins, Spry2 and Dyrk1A, was measured in protein homogenates obtained from the hippocampus of control and HHcy mice. Results showed that Spry2 protein was upregulated, whereas Dyrk1A protein was downregulated, in the hippocampus of Hcy-treated mice when compared to vehicle-treated control mice (Fig. 3 D-F). In summary, high Hcy levels altered the expression of both Spry2 and Dyrk1A in the hippocampus *in vivo*.

3.8. Spry2 overexpression reduces NPC proliferation

To test whether Spry2 overexpression alone was enough to reduce bFGF-dependent NPC proliferation, these cells were transfected with a pcDNA3.3 vector encoding Spry2 under the control of the CMV promoter. Transfection of NPC with pcDNA3.3/Spry2 resulted in a nearly 3-fold increase on Spry2 expression, as detected by western blot (Fig. 4 A), and an almost 35% reduction in the percentage of cells undergoing cell cycle

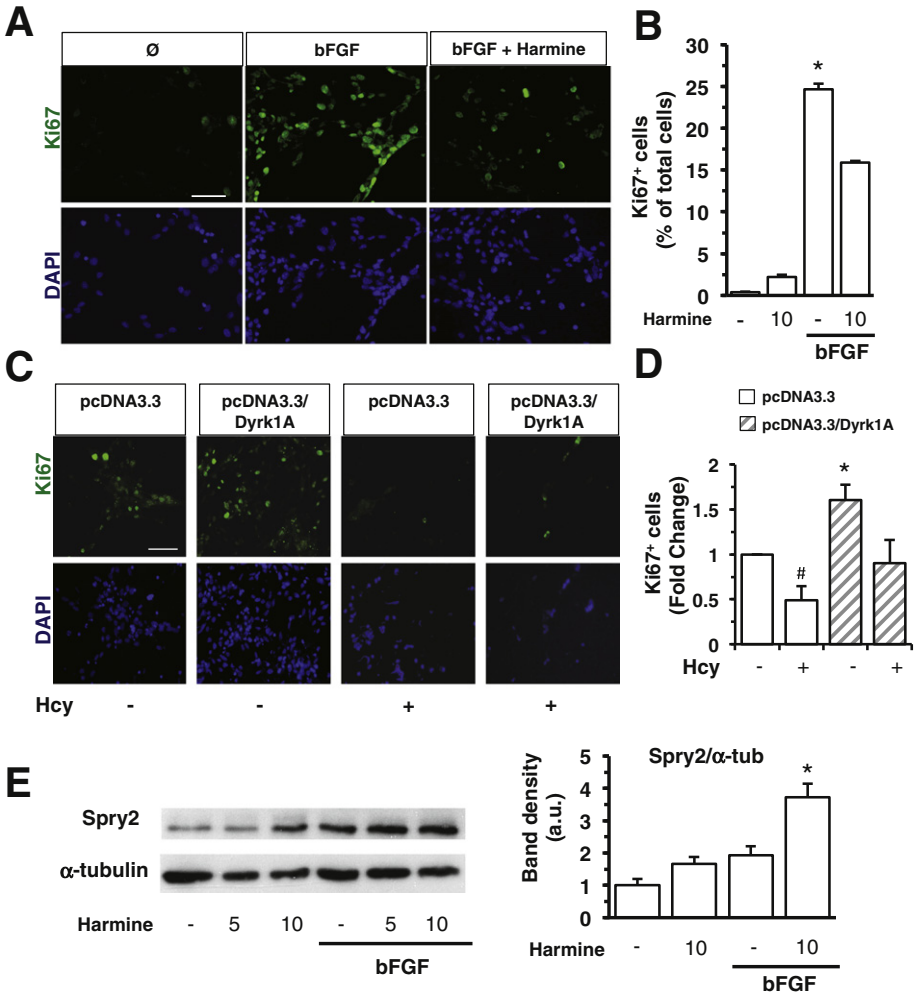

Fig. 5. Inhibition of Dyrk1A activity by Hcy modulates Spry2 concentration and NPC proliferation. (**A**) Representative fluorescence microscopy images obtained from immunodetection of Ki67 (green) and DAPI staining (blue) in NPC cultures adhered on PLO and stimulated with or without bFGF for 24 h in the presence and absence of the Dyrk1A inhibitor harmine (10 μM). (**B**) Quantification of the percentage of Ki67$^+$ cells in the culture conditions explained in A; (*) means statistically significant compared to rest of groups. (C) Representative fluorescence microscopy images obtained from immunodetection of Ki67 (green) and DAPI staining (blue) in NPC cultures adhered on PLO, transfected with either an empty pcDNA3.3 vector or a pcDNA3.3 vector expressing Dyrk1A (pcDNA3.3/Dyrk1A) and stimulated with bFGF for 24 h, in the presence and absence of Hcy. Scale bar 50 μM (D) Quantification of Ki67$^+$ cells in the culture conditions explained in C; Ki67$^+$ cells are expressed as percentage of total cells and made relative to the mock-transfected condition; (*) means statistically significant compared to rest of groups; (#) means statistically significant compared to pcDNA3.3-transfected cells in the absence of Hcy. (E) Representative autoradiographic images and quantification of immunoblots to detect Spry2 in cultures stimulated with or without bFGF and different concentrations of the Dyrk1A inhibitor harmine. Harmine was added to the cultures 3 h before bFGF stimulation and cells were lysed 4 h after bFGF addition. Results are the average ± SE of three independent experiments; (*) means statistically significant ($p < 0.05$) compared to rest of groups.

(Ki67$^+$ cells) (Fig. 4 B-C). Thus, exogenous overexpression of Spry2 was sufficient to inhibit neural progenitor cell proliferation.

3.9. The repressing effect of Spry2 on FGFR signaling and NPC proliferation is modulated by Dyrk1A activity

To further analyze the role of Dyrk1A in bFGF-driven NPC proliferation, NPC cultures were stimulated with bFGF in the presence or absence of the Dyrk1A specific inhibitor harmine [38] and proliferation was analyzed afterwards. The percentage of Ki67$^+$ cells in cultures treated with harmine dropped to 64% of the observed in non-treated cultures (Fig. 5 A, B), indicating that inhibition of Dyrk1A activity reduced bFGF-stimulated proliferation.

The effect of Dyrk1A inhibition by harmine on Spry2 protein levels was studied in NPC cultures. In the presence of bFGF, a 2-fold increase on dephospho-Spry2 was observed in harmine-treated cultures compared to control cultures (Fig. 5 E), indicating that Dyrk1A inhibition maintained Spry2 in a dephosphorylated state, protecting it from proteasomal degradation. Thus, both harmine and Hcy were able to negatively act on Dyrk1A to increase Spry2 protein levels, the former by direct Dyrk1A inhibition and the latter by Dyrk1A protein downregulation, and the common outcome was dephospho-Spry2 levels, which repressed bFGF signaling resulting in a significant reduction on NPC proliferation.

Dyrk1A was cloned into a pcDNA3.3 mammalian expression vector and transfected into NPC cultures, in order to test whether overexpression of Dyrk1A exerted an effect on bFGF-mediated NPC proliferation. Transfection of bFGF-treated NPC cultures with the pcDNA3.3/Dyrk1A vector increased the percentage of cycling Ki67$^+$ cells to 160% compared to cultures transfected with the empty vector (Fig. 5 C-D), suggesting that Spry2 phosphorylation by excessive Dyrk1A was derepressing the FGFR proliferation signal. However, Dyrk1A overexpression did not completely protect NPC from the inhibitory effect of Hcy on NPC proliferation (Fig. 5 C-D), This result prompted as to investigate whether another mechanism induced by Hcy was counteracting Dyrk1A activity.

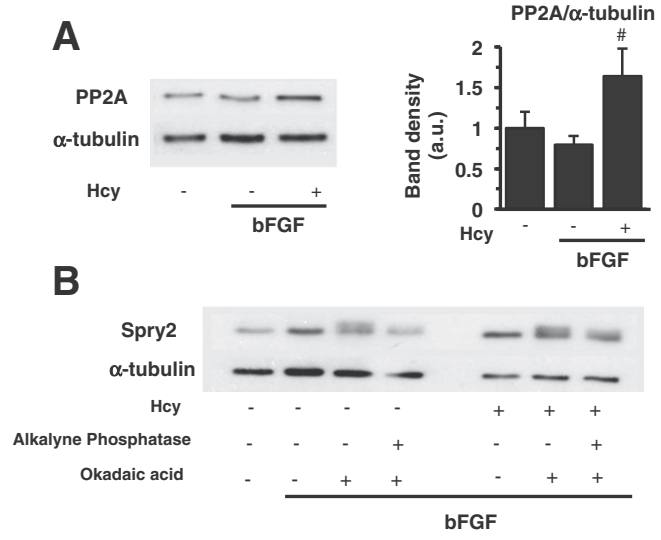

Fig. 6. PP2Ac is upregulated in Hcy-treated NPC cultures. (**A**) Representative autoradiographic images of immunoblot bands detecting de catalytic subunit of Spry2 phosphatase PP2A (PP2Ac) and α-tubulin in cultures stimulated with bFGF in the presence and absence of Hcy, and densitometric quantification of bands expressed as the ratio PP2Ac/α-tubulin. Cells were treated with or without 100 μM Hcy 1.5 h prior to bFGF addition, and were lysed 3 h after bFGF stimulation. Results are the average ± SE of four independent experiments; (#) $p < 0.05$ compared to cultures in the absence of Hcy. (**B**) Representative autoradiographic images of western blot immunodetection of Spry2 in NPC exposed to the indicated conditions. Cells were treated with or without 100 μM Hcy and 100 nM okadaic acid 1.5 h prior to bFGF addition, and were lysed 3 h after bFGF stimulation. Alkaline phosphatase treatment was performed in cell lysates for 30 min at 37 °C.

3.10. PP2Ac is upregulated in the presence of Hcy

In an attempt to further understand how Spry2 dephosphorylation occurred in neural precursors, we analyzed the expression of the Spry2-phosphatase PP2A catalytic subunit (PP2Ac), which has been described to dephosphorylate Spry2 in serine residues 115 and 118 [21]. NPC cultures were stimulated for 3 h with bFGF, in the presence and absence of Hcy. We observed a 2 fold increase on PP2Ac expression in Hcy-treated cultures compared to controls (Fig. 6 A). In addition, we analyzed how PP2Ac activity was related to Spry2 dephosphorylation by using okadaic acid, a PP2A inhibitor. Cultures stimulated with bFGF were treated with okadaic acid in the presence and absence of Hcy. In the presence of okadaic acid, a second Spry2 band corresponding to phospho-Spry2 appeared, and this form was eliminated by alkaline phosphatase treatment; a similar effect was observed when cultures were treated with Hcy (Fig. 6 B), indicating that increased PP2A may facilitate the dephosphorylation and stabilization of Spry2 triggered by Hcy.

4. Discussion

It has been previously shown that Hcy inhibits FGFR-mediated (but not EGFR-mediated) Erk1/2 phosphorylation in postnatal NPC, leading to downstream consequences such as cyclin E downregulation and proliferation arrest [6]; however, the molecular mechanisms involved remained to be investigated. In this work, we have found that Spry2 is a key molecule in the regulation of cell cycle progression in NPC in response to bFGF; we have also found that the expression and activity of Spry2 is modified by Hcy and by other metabolites that alter the cellular methylation potential. Our proposed model for the interaction between Hcy and Spry2 is synthesized in the diagram shown in Fig. 7. Spry2 is a potent endogenous inhibitor of FGFR-Erk1/2 signaling that specifically interferes with the MAPK pathway without affecting Akt or other kinases activated by growth factor receptors. Spry2 function is essential for many aspects of development, but its role in the adult mammalian brain has scarcely been investigated. Given the importance of bFGF signaling in adult neurogenesis and NPC proliferation, it was not surprising to find that Spry2 is involved in the regulation of these processes. The work presented in here demonstrates that Spry2 regulates proliferation in NPC, likely by switching off the FGFR-Erk1/2 signaling cascade. We have observed, in NPC cultures, that, once signaling through FGFR-Erk1/2 is activated by bFGF, Spry2 mRNA is upregulated transiently during the first 3 h —presumably to enhance Spry2 activity—, dropping back to basal levels 8 h after bFGF stimulation. However, we also show that under certain conditions such as the presence of elevated Hcy or methyltransferase inhibitors, the rise in Spry2 levels occurs faster, is more pronounced, and is prolonged for at least 24 h, impairing the proliferative response of NPC to bFGF. We

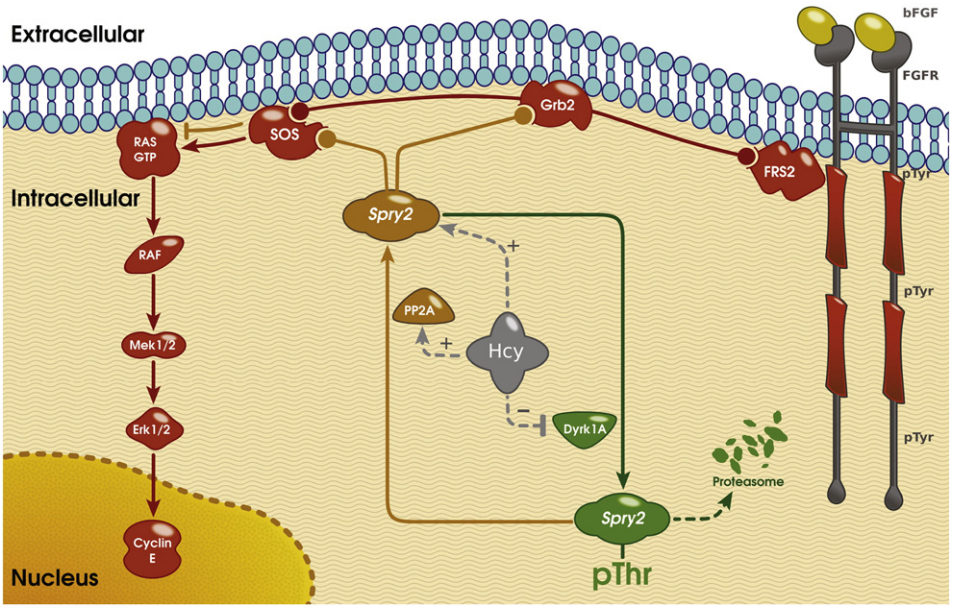

Fig. 7. Proposed model for the interaction between Hcy, Spry2, and the FGFR-MAPK signaling cascade in NPC. Diagram shows the intracellular FGFR-Erk1/2-cyclin E signaling pathway in NPC (red elements), and depicts how Spry2 interacts with components of this pathway in order to inhibit it. The inhibitory activity of Spry2 depends on protein regulation by phosphorylation via Dyrk1A (green) and dephosphorylation via PP2A (yellow), as indicated. The molecular elements affected by Hcy (gray) are indicated.

have identified some of the molecular mechanisms underlying this impairment, which include Spry2 promoter demethylation, Spry2 upregulation and activation by dephosphorylation, downregulation of the Spry2-deactivating kinase Dyrk1A, and upregulation of the Spry2 phosphatase PP2A.

4.1. Intracellular Spry2 is transiently upregulated by bFGF

The bFGF-FGFR-Erk1/2 pathway stimulates proliferation in NPC by inducing cyclin E expression [6]. Spry2 negatively regulates the activation of this FGFR-Erk1/2 signaling pathway by switching off cascade activation [39]. We have found that Spry2 mRNA expression rises fast upon stimulation of NPC with bFGF presumably to switch off the FGFR-Erk1/2 signaling cascade but only for a short period of time. This Spry2 mRNA upregulation was followed by a small, but not statistically significant, increase on Spry2 protein expression. One possible explanation for such a small change in Spry2 protein levels (albeit a pronounced mRNA increase) in response to bFGF is that this growth factor, as we will discuss later on, concomitantly stimulated Spry2 degradation via the proteasome.

4.2. Elevated levels of Hcy exacerbate Spry2 expression and FGFR signaling inhibition

Our results show that the molecular mechanisms underlying the inhibition of the FGFR-MAPK signaling pathway in the presence of Hcy include an aberrant Spry2 upregulation, at both protein and mRNA levels. In the presence of Hcy, the transient 3-fold increase on Spry2 mRNA was abnormally sustained 8 h after bFGF stimulation, and kept increasing further up at longer periods of time. This persistence in Spry2 mRNA expression in the presence of Hcy can be attributed to the observed Spry2 promoter demethylation (Fig. 1 F, G), which is also observed in the presence of the methyltransferase activity inhibitor AdOx [40,41] (Fig. 1 H), indicating that the effect of Hcy on Spry2 promoter demethylation is likely mediated by its capacity to inhibit methyltransferases [42]. In support of this idea, treatment with AdOx not only induced Spry2 promoter demethylation, but it also mimicked all of the reported effects of Hcy in NPC cultures: inhibition of Erk1/2 activity, downregulation of cyclin E expression, and reduction of NPC proliferation (Fig. 2).

We also show that the fast raise in Spry2 protein levels found in the presence of Hcy shortly after bFGF stimulation is a consequence of the increased protein stabilization through dephosphorylation (Fig. 3 A). Spry2 repressing activity is limited by phosphorylation-dependent complex formation with the adaptor protein c-Cbl, which recruits E3 ubiquitin ligase and mediates Spry2 polyubiquitination and degradation in the proteasome (Reviewed in [22]). In bFGF-treated NPC cultures, the phosphorylated form of Spry2 was only detectable in the presence of the proteasome inhibitor lactacystin (Fig. 3 A), indicating that phosphorylated Spry2 is readily degraded in NPC in response to bFGF. After a short exposure to Hcy, however, the ratio dephospho/phospho Spry2 increased by two fold, and so did the Spry2 stabilization and activity.

In conclusion, inhibition of methyltransferase activity by adding either high Hcy or Adox to NPC results in Spry2 promoter demethylation, sustained Spry2 protein expression and stability in response to bFGF, and chronic inactivation of the FGFR-Erk1/2 signaling.

4.3. Altered expression of Dyrk1A kinase and PP2A phosphatase underlie Spry2 posttranslational modifications in response to Hcy

The increase on Spry2 protein stability induced by Hcy needed further explanations beyond just promoter demethylation. To investigate molecular mechanisms implied in Spry2 stability, we focused on two enzymes –PP2A phosphatase and Dyrk1A kinase– that play important roles in Spry2 activation/inactivation, respectively. Dyrk1A is a serine/threonine kinase that phosphorylates Spry2 in Thr75, increasing the degradation of this negative regulator of FGFR signaling [23]. Interestingly, Dyrk1A has been found misregulated in the liver of hyperhomocysteinemic mice, affecting the MAPK-Erk1/2 pathway [43]. Additionally, an adequate dosage of Dyrk1A determines neuronal differentiation of NPC during development and alterations in this dosage impair CNS development. This occurs in individuals with Down syndrome in which Dyrk1A gene is triplicated leading to an elevated dosage of these protein [27]. On the contrary, Spry2 dephosphorylation mediated by PP2A facilitates its binding to Grb2, which leads to FGFR-Erk1/2 inhibition [28–31]. We have found that treatment of NPC with high Hcy results in a significant reduction in intracellular Dyrk1A levels (Fig. 3 B) and a large increase on the amount of phosphatase PP2A (Fig. 6 A), both of which are likely contributing to the accumulation of the stable dephospho-Spry2 observed in NPC cultures after Hcy treatment. In fact, Dyrk1A inhibition with harmine results in increased Spry2 protein levels (Fig. 5 E), while the western-blot bands corresponding to dephospho-Spry2 vanished in the presence of the PP2Ac inhibitor okadaic acid (Fig. 6 B).

Spry2 controls proliferation in other types of cells [44,45], and it is considered a tumor suppressor protein. It has been found to be downregulated in several types of cancer [24–26], including the non-small cell lung cancer, contributing to tumor malignancy [44]. It is plausible that the knowledge brought about by this and other works may help restrain Spry2 downregulation in certain types of tumors.

We have been unable to determine the role of PP2A on NPC proliferation, since the inhibition of PP2Ac with okadaic acid completely impaired the capacity of NPC to grow in culture. In contrast, the crucial importance of Dyrk1A activity for bFGF-induced NPC proliferation has been clearly shown in here. Dyrk1A inhibition by treatment with harmine [38] significantly decreased bFGF-dependent NPC proliferation, likely due to increased half-life and activity of Spry2. In support of this idea, the antiproliferative effect of high levels of Spry2 induced by Hcy treatment was reverted by Dyrk1A overexpression. These findings agree with previous reports showing that the interaction Dyrk1A–Spry2 controls Spry2 phosphorylation and degradation [20].

Dyrk1A has specifically been implicated in some important aspects of NPC function [46]; during asymmetric division of neural stem cells, Dyrk1A is segregated to only one of the daughter cells: the one with the strongest proliferative capacity. We can now hypothesize that Dyrk1A levels in the progeny of neural stem cells will inversely correlate with Spry2 levels and, if this was the case, the lack of Dyrk1A in the other daughter cell obtained after asymmetric division could make it resistant to growth factor stimulation due to high levels of Spry2, and thus, prone to quiescence.

We have indeed found an inverse correlation between Dyrk1A and Spry2 levels in the hippocampus of HHcy mice. An elevated concentration of Spry2 and a reduced concentration of Dyrk1A was observed in this mouse model of moderate HHcy, obtained by chronic Hcy infusion, in which it has been previously demonstrated that neurogenesis is impaired in both the SVZ and DG [6]. These *in vivo* results are in agreement with the *in vitro* effects of Hcy on Dyrk1A and Spry2 expression in NPC cultures. A previous report by Abekhouk *et al.* shows conflicting data regarding cystathionine beta synthase (CBS)-deficient mice, a different model of HHcy mice, in which Dyrk1A protein is slightly upregulated and Spry2 slightly downregulated in whole brain extracts [32], contrary to what we show in the hippocampus of our animal model. We believe that our results differ from those of Abekhouk *et al.* because we have analyzed Dyrk1A and Spry2 expression specifically in hippocampal extracts, and not in whole brain lysates. Remarkably, a previous report from our lab shows that methionine metabolism is regulated differently in the hippocampus as compared to other parts of the brain: the liver enzyme Glycine-N-methyltransferase (GNMT), which regulates cellular SAM/SAH ratios, is specifically expressed within the hippocampus and not in other brain regions [15]. Methionine metabolism is important not only in the liver, but also in those specific tissues where epigenetic plasticity (namely, methylation reactions) occurs, like the hippocampus, where

epigenetic changes in response to environmental cues have been reported [47,48]. Accordingly, the CBS-deficient mice described by Abekhoukh et al. [32] do exhibit increased levels of Spry2 and decreased levels of Dyrk1A in the liver, which is in agreement to what we see in the hippocampus of HHcy mice. Thus, in the specific tissues where GNMT is expressed, Spry2 and Dyrk1A expression varies similarly, and our hypothesis is that the hippocampus of CBS-deficient mice might not behave as the whole brain. The one question that remains to be solved is how Hcy alters Dyrk1A and PP2A expression in opposite directions. The reduction in Dyrk1A protein observed in NPC cultures after treatment with Hcy was concomitant with a paradoxical upregulation of Dyrk1A mRNA expression. This apparent contradiction suggests that Hcy might be exerting a strong post-transcriptional or posttranslational effect that results in low levels of Dyrk1A protein albeit increased mRNA. Translation in eukaryotes can start at the 5′ end of the mRNA, where the 7-methylguanosine cap structure is (cap-dependent initiation), or internally within the 5'UTR (cap-independent initiation). Formation of the 7-methylguanosine cap occurs in two reactions as the substrate mRNA is being transcribed, the first catalyzed by the enzyme RNA guanylyl transferase and 5′ triphosphatase (RNGTT) and the second by the enzyme RNA guanine 7-methylguanosine transferase (RNMT), which transfers methyl groups from SAM to guanosines in the cap structure. This latter reaction can be inhibited by SAH accumulation when SAHH does not hydrolyze SAH to Hcy and adenosine (which happens when Hcy levels are high, see Fig. 1 H) [49]. There are no evidences to date that indicate that Dyrk1A translation might be modulated by mRNA methylation. However, it seems reasonable to hypothesize that Dyrk1A translation might be facilitated when its mRNA is cap-methylated, and that HHcy-induced accumulation of SAH might inhibit this methylation reaction, reducing Dyrk1A mRNA translation. A final consideration is that differential regulation of translation can generate protein gradients within a single cell, or the asymmetrical distribution of a protein between sibling cells during cell division [50]. As stated before, this is the case for Dyrk1A during neural stem cell asymmetric division, and this should be considered when studying the impact that HHcy may have in neural stem cell self-renewal capacity and neurogenesis.

Our results show the means by which metabolic alterations that have an impact on the cellular methylation potential might impair bFGF-stimulated proliferation of NPC and adult neurogenesis, which include direct upregulation of Spry2 expression and an indirect stabilization of Spry2 by altering the concentrations of Dyrk1A and PP2A, leading to further activation of Srpy2.

Supplementary data to this article can be found online at http://dx.doi.org/10.1016/j.bbamcr.2016.09.018.

Funding

This work was funded by the Spanish Ministerio de Economía y Competitividad MINNECO (grant number: SAF2008–03,879 and BFU2015–68,652-R), by the Consejería de Economía Innovación, Ciencia y Empleo, Junta de Andalucía, Spain (grant numbers P10-CTS6639 P11-CTS-7847), and by Fundación Rodríguez Pascual 2015 grants.

Transparency document

The Transparency document associated with this article can be found, in online version.

Acknowledgments

We thank the animal facility (SEPA) of the University of Cádiz for their support, and Juan Antonio Muñoz Berraquero for help in the design of the illustration in Fig. 7.

References

[1] H. Refsum, P.M. Ueland, O. Nygard, S.E. Vollset, Homocysteine and cardiovascular disease, Annu. Rev. Med. 49 (1998) 31–62.
[2] S. Seshadri, A. Beiser, J. Selhub, P.F. Jacques, I.H. Rosenberg, R.B. D'Agostino, P.W. Wilson, P.A. Wolf, Plasma homocysteine as a risk factor for dementia and Alzheimer's disease, N. Engl. J. Med. 346 (2002) 476–483.
[3] G. Ravaglia, P. Forti, F. Maioli, M. Chiappelli, F. Montesi, E. Tumini, E. Mariani, F. Licastro, C. Patterson, Blood inflammatory markers and risk of dementia: The Conselice Study of Brain Aging, Neurobiol. Aging (2006).
[4] M.N. Haan, J.W. Miller, A.E. Aiello, R.A. Whitmer, W.J. Jagust, D.M. Mungas, L.H. Allen, R. Green, Homocysteine, B vitamins, and the incidence of dementia and cognitive impairment: results from the Sacramento Area Latino Study on Aging, Am. J. Clin. Nutr. 85 (2007) 511–517.
[5] V. Lerner, C. Miodownik, A. Kaptsan, T. Vishne, B.A. Sela, J. Levine, High serum homocysteine levels in young male schizophrenic and schizoaffective patients with tardive parkinsonism and/or tardive dyskinesia, J. Clin. Psychiatry 66 (2005) 1558–1563.
[6] L.G. Rabaneda, M. Carrasco, M.A. Lopez-Toledano, M. Murillo-Carretero, F.A. Ruiz, C. Estrada, C. Castro, Homocysteine inhibits proliferation of neuronal precursors in the mouse adult brain by impairing the basic fibroblast growth factor signaling cascade and reducing extracellular regulated kinase 1/2-dependent cyclin E expression, FASEB J. 22 (2008) 3823–3835.
[7] S. Lugert, O. Basak, P. Knuckles, U. Haussler, K. Fabel, M. Gotz, C.A. Haas, G. Kempermann, V. Taylor, C. Giachino, Quiescent and active hippocampal neural stem cells with distinct morphologies respond selectively to physiological and pathological stimuli and aging, Cell Stem Cell 6 (2010) 445–456.
[8] L.C. Fuentealba, K. Obernier, A. Alvarez-Buylla, Adult neural stem cells bridge their niche, Cell Stem Cell 10 (2012) 698–708.
[9] G.L. Ming, H. Song, Adult neurogenesis in the mammalian brain: significant answers and significant questions, Neuron 70 (2011) 687–702.
[10] S. Goldman, Glia as neural progenitor cells, Trends Neurosci. 26 (2003) 590–596.
[11] A. Alvarez-Buylla, J.M. Garcia-Verdugo, Neurogenesis in adult subventricular zone, J. Neurosci. 22 (2002) 629–634.
[12] T.D. Palmer, J. Ray, F.H. Gage, FGF-2-responsive neuronal progenitors reside in proliferative and quiescent regions of the adult rodent brain, Mol. Cell. Neurosci. 6 (1995) 474–486.
[13] K. Jin, Y. Sun, L. Xie, S. Batteur, X.O. Mao, C. Smelick, A. Logvinova, D.A. Greenberg, Neurogenesis and aging: FGF-2 and HB-EGF restore neurogenesis in hippocampus and subventricular zone of aged mice, Aging Cell 2 (2003) 175–183.
[14] N.D. Bull, P.F. Bartlett, The adult mouse hippocampal progenitor is neurogenic but not a stem cell, J. Neurosci. 25 (2005) 10815–10821.
[15] M. Carrasco, L.G. Rabaneda, M. Murillo-Carretero, S. Ortega-Martinez, M.L. Martinez-Chantar, A. Woodhoo, Z. Luka, C. Wagner, S.C. Lu, J.M. Mato, J.A. Mico, C. Castro, Glycine N-methyltransferase expression in the hippocampus and its role in neurogenesis and cognitive performance, Hippocampus 24 (2014) 840–852.
[16] H. Hanafusa, S. Torii, T. Yasunaga, E. Nishida, Sprouty1 and Sprouty2 provide a control mechanism for the Ras/MAPK signalling pathway, Nat. Cell Biol. 4 (2002) 850–858.
[17] D.G. Yim, S. Ghosh, G.R. Guy, D.M. Virshup, Casein kinase 1 regulates Sprouty2 in FGF-ERK signaling, Oncogene 34 (2015) 474–484.
[18] J. DaSilva, L. Xu, H.J. Kim, W.T. Miller, D. Bar-Sagi, Regulation of sprouty stability by Mnk1-dependent phosphorylation, Mol. Cell. Biol. 26 (2006) 1898–1907.
[19] S. Chandramouli, C.Y. Yu, P. Yusoff, D.H. Lao, H.F. Leong, K. Mizuno, G.R. Guy, Tesk1 interacts with Spry2 to abrogate its inhibition of ERK phosphorylation downstream of receptor tyrosine kinase signaling, J. Biol. Chem. 283 (2008) 1679–1691.
[20] S. Aranda, M. Alvarez, S. Turro, A. Laguna, S. de la Luna, Sprouty2-mediated inhibition of fibroblast growth factor signaling is modulated by the protein kinase DYRK1A, Mol. Cell. Biol. 28 (2008) 5899–5911.
[21] D.H. Lao, P. Yusoff, S. Chandramouli, R.J. Philp, C.W. Fong, R.A. Jackson, T.Y. Saw, C.Y. Yu, G.R. Guy, Direct binding of PP2A to Sprouty2 and phosphorylation changes are a prerequisite for ERK inhibition downstream of fibroblast growth factor receptor stimulation, J. Biol. Chem. 282 (2007) 9117–9126.
[22] J.M. Mason, D.J. Morrison, M.A. Basson, J.D. Licht, Sprouty proteins: multifaceted negative-feedback regulators of receptor tyrosine kinase signaling, Trends Cell Biol. 16 (2006) 45–54.
[23] C.E. Mayer, B. Haigl, F. Jantscher, G. Siegwart, M. Grusch, W. Berger, H. Sutterluty, Bimodal expression of Sprouty2 during the cell cycle is mediated by phase-specific Ras/MAPK and c-Cbl activities, Cell. Mol. Life Sci. 67 (2010) 3299–3311.
[24] A.B. McKie, D.A. Douglas, S. Olijslagers, J. Graham, M.M. Omar, R. Heer, V.J. Gnanapragasam, C.N. Robson, H.Y. Leung, Epigenetic inactivation of the human sprouty2 (hSPRY2) homologue in prostate cancer, Oncogene 24 (2005) 2166–2174.
[25] T.L. Lo, P. Yusoff, C.W. Fong, K. Guo, B.J. McCaw, W.A. Phillips, H. Yang, E.S. Wong, H.F. Leong, Q. Zeng, T.C. Putti, G.R. Guy, The ras/mitogen-activated protein kinase pathway inhibitor and likely tumor suppressor proteins, sprouty 1 and sprouty 2 are deregulated in breast cancer, Cancer Res. 64 (2004) 6127–6136.
[26] C.W. Fong, M.S. Chua, A.B. McKie, S.H. Ling, V. Mason, R. Li, P. Yusoff, T.L. Lo, H.Y. Leung, S.K. So, G.R. Guy, Sprouty 2, an inhibitor of mitogen-activated protein kinase signaling, is down-regulated in hepatocellular carcinoma, Cancer Res. 66 (2006) 2048–2058.
[27] M. Hattori, A. Fujiyama, T.D. Taylor, H. Watanabe, T. Yada, H.S. Park, A. Toyoda, K. Ishii, Y. Totoki, D.K. Choi, Y. Groner, E. Soeda, M. Ohki, T. Takagi, Y. Sakaki, S. Taudien, K. Blechschmidt, A. Polley, U. Menzel, J. Delabar, K. Kumpf, R. Lehmann, D. Patterson, K. Reichwald, A. Rump, M. Schillhabel, A. Schudy, W. Zimmermann, A. Rosenthal, J. Kudoh, K. Schibuya, K. Kawasaki, S. Asakawa, A. Shintani, T. Sasaki, K. Nagamine, S. Mitsuyama, S.E. Antonarakis, S. Minoshima, N. Shimizu, G. Nordsiek, K. Hornischer, P. Brant, M. Scharfe, O. Schon, A. Desario, J. Reichelt, G.

Kauer, H. Blocker, J. Ramser, A. Beck, S. Klages, S. Hennig, L. Riesselmann, E. Dagand, T. Haaf, S. Wehrmeyer, K. Borzym, K. Gardiner, D. Nizetic, F. Francis, H. Lehrach, R. Reinhardt, M.L. Yaspo, m. Chromosome, c. sequencing, The DNA sequence of human chromosome 21, Nature 405 (2000) 311–319.
[28] F. Guedj, P.L. Pereira, S. Najas, M.J. Barallobre, C. Chabert, B. Souchet, C. Sebrie, C. Verney, Y. Herault, M. Arbones, J.M. Delabar, DYRK1A: a master regulatory protein controlling brain growth, Neurobiol. Dis. 46 (2012) 190–203.
[29] B. Souchet, F. Guedj, I. Sahun, A. Duchon, F. Daubigney, A. Badel, Y. Yanagawa, M.J. Barallobre, M. Dierssen, E. Yu, Y. Herault, M. Arbones, N. Janel, N. Creau, J.M. Delabar, Excitation/inhibition balance and learning are modified by Dyrk1a gene dosage, Neurobiol. Dis. 69 (2014) 65–75.
[30] A. Thomazeau, O. Lassalle, J. Iafrati, B. Souchet, F. Guedj, N. Janel, P. Chavis, J. Delabar, O.J. Manzoni, Prefrontal deficits in a murine model overexpressing the down syndrome candidate gene dyrk1a, J. Neurosci. 34 (2014) 1138–1147.
[31] S. Najas, J. Arranz, P.A. Lochhead, A.L. Ashford, D. Oxley, J.M. Delabar, S.J. Cook, M.J. Barallobre, M.L. Arbones, DYRK1A-mediated Cyclin D1 Degradation in Neural Stem Cells Contributes to the Neurogenic Cortical Defects in Down Syndrome, EBioMedicine 2 (2015) 120–134.
[32] S. Abekhoukh, C. Planque, C. Ripoll, P. Urbaniak, J.L. Paul, J.M. Delabar, N. Janel, Dyrk1A, a serine/threonine kinase, is involved in ERK and Akt activation in the brain of hyperhomocysteinemic mice, Mol. Neurobiol. 47 (2013) 105–116.
[33] J.D. Finkelstein, W.E. Kyle, B.J. Harris, Methionine metabolism in mammals: regulatory effects of S-adenosylhomocysteine, Arch. Biochem. Biophys. 165 (1974) 774–779.
[34] T.A. Garrow, Purification, kinetic properties, and cDNA cloning of mammalian betaine-homocysteine methyltransferase, J. Biol. Chem. 271 (1996) 22831–22838.
[35] A. Torroglosa, M. Murillo-Carretero, C. Romero-Grimaldi, E.R. Matarredona, A. Campos-Caro, C. Estrada, Nitric oxide decreases subventricular zone stem cell proliferation by inhibition of epidermal growth factor receptor and phosphoinositide-3-kinase/Akt pathway, Stem Cells 25 (2007) 88–97.
[36] J. Winer, C.K. Jung, I. Shackel, P.M. Williams, Development and validation of real-time quantitative reverse transcriptase-polymerase chain reaction for monitoring gene expression in cardiac myocytes in vitro, Anal. Biochem. 270 (1999) 41–49.
[37] G.R. Guy, R.A. Jackson, P. Yusoff, S.Y. Chow, Sprouty proteins: modified modulators, matchmakers or missing links? J. Endocrinol. 203 (2009) 191–202.
[38] N. Gockler, G. Jofre, C. Papadopoulos, U. Soppa, F.J. Tejedor, W. Becker, Harmine specifically inhibits protein kinase DYRK1A and interferes with neurite formation, FEBS J. 276 (2009) 6324–6337.
[39] T. Casci, J. Vinos, M. Freeman, Sprouty, an intracellular inhibitor of Ras signaling, Cell 96 (1999) 655–665.
[40] R.B. Pilz, G. Van den Berghe, G.R. Boss, Adenosine dialdehyde and nitrous oxide induce HL-60 differentiation, Blood 70 (1987) 1161–1164.
[41] B.A. Johnson, J. Najbauer, D.W. Aswad, Accumulation of substrates for protein L-isoaspartyl methyltransferase in adenosine dialdehyde-treated PC12 cells, J. Biol. Chem. 268 (1993) 6174–6181.
[42] G.L. Cantoni, Biological methylation: selected aspects, Annu. Rev. Biochem. 44 (1975) 435–451.
[43] J. Hamelet, C. Noll, C. Ripoll, J.L. Paul, N. Janel, J.M. Delabar, Effect of hyperhomocysteinemia on the protein kinase DYRK1A in liver of mice, Biochem. Biophys. Res. Commun. 378 (2009) 673–677.
[44] H. Sutterluty, C.E. Mayer, U. Setinek, J. Attems, S. Ovtcharov, M. Mikula, W. Mikulits, M. Micksche, W. Berger, Down-regulation of Sprouty2 in non-small cell lung cancer contributes to tumor malignancy via extracellular signal-regulated kinase pathway-dependent and -independent mechanisms, Mol. Cancer Res. 5 (2007) 509–520.
[45] T. Sanui, U. Tanaka, T. Fukuda, K. Toyoda, T. Taketomi, R. Atomura, K. Yamamichi, F. Nishimura, Mutation of Spry2 induces proliferation and differentiation of osteoblasts but inhibits proliferation of gingival epithelial cells, J. Cell. Biochem. 116 (2015) 628–639.
[46] S.R. Ferron, N. Pozo, A. Laguna, S. Aranda, E. Porlan, M. Moreno, C. Fillat, S. de la Luna, P. Sanchez, M.L. Arbones, I. Farinas, Regulated segregation of kinase Dyrk1A during asymmetric neural stem cell division is critical for EGFR-mediated biased signaling, Cell Stem Cell 7 (2010) 367–379.
[47] X. Zhao, T. Ueba, B.R. Christie, B. Barkho, M.J. McConnell, K. Nakashima, E.S. Lein, B.D. Eadie, A.R. Willhoite, A.R. Muotri, R.G. Summers, J. Chun, K.F. Lee, F.H. Gage, Mice lacking methyl-CpG binding protein 1 have deficits in adult neurogenesis and hippocampal function, Proc. Natl. Acad. Sci. U. S. A. 100 (2003) 6777–6782.
[48] D.K. Ma, M.H. Jang, J.U. Guo, Y. Kitabatake, M.L. Chang, N. Pow-Anpongkul, R.A. Flavell, B. Lu, G.L. Ming, H. Song, Neuronal activity-induced Gadd45b promotes epigenetic DNA demethylation and adult neurogenesis, Science 323 (2009) 1074–1077.
[49] M.E. Fernandez-Sanchez, T. Gonatopoulos-Pournatzis, G. Preston, M.A. Lawlor, V.H. Cowling, S-adenosyl homocysteine hydrolase is required for Myc-induced mRNA cap methylation, protein synthesis, and cell proliferation, Mol. Cell. Biol. 29 (2009) 6182–6191.
[50] J.J. Wolf, R.D. Dowell, S. Mahony, M. Rabani, D.K. Gifford, G.R. Fink, Feed-forward regulation of a cell fate determinant by an RNA-binding protein generates asymmetry in yeast, Genetics 185 (2010) 513–522.